# SOFT ANOMALOUS DIMENSION MATRICES IN HEAVY QUARK–ANTIQUARK HADROPRODUCTION IN ASSOCIATION WITH A GLUON JET*

E. Szarek

Institute of Physics, Jagiellonian University
Łojasiewicza 11, 30-348 Kraków, Poland
e.szarek@th.if.uj.edu.pl

*(Received August 30, 2018; accepted October 12, 2018)*

We compute the soft anomalous dimension (SAD) matrices for production of massive quarks $Q$ and $\bar{Q}$ in association with a gluon jet, from massless quarks $q$ and antiquarks $\bar{q}$: $q\bar{q} \to Q\bar{Q}g$, and in the gluon scattering $gg \to Q\bar{Q}g$. To analyse the behaviour of the eigenvalues of SAD matrices, we perform numerical studies of their eigensystems at two special kinematical configurations.

DOI:10.5506/APhysPolB.49.1839

## 1. Introduction

The motivation of this paper is dictated by the interest in the precision physics at the Large Hadron Collider (LHC). Providing precise theory predictions for the Standard Model processes is necessary to fully explore a physics potential of the LHC. One of the key point of the LHC physics program are studies of the heaviest particle of the Standard Model, that is the top quark. In particular, the top-quark production may occur in the $t\bar{t}$ channel in association with an additional jet. It is difficult to calculate perturbative fixed order QCD corrections for the processes with 3 particles in the final state. Soft-gluon resummation offers possibility to systematically improve the precision of calculations. The necessary ingredient of the soft-gluon resummation are the soft anomalous dimension (SAD) matrices. Hence, we calculate the SAD matrices for a general case of a heavy quark–antiquark production with a gluon jet. This paper contributes to ongoing activity to effectively apply soft-gluon resummation to $2 \to 3$ processes [1–6]. The obtained results open the way for numerical calculations of the improved cross sections.

In QCD, one finds infrared divergences in perturbative corrections: soft collinear, collinear and soft non-collinear. The collinear divergences appear when the angle between momenta of two external massless partons $\theta \to 0$. The soft divergences occur for an emitted gluon energy $E \to 0$. After the procedure of regularization, the IR divergences cancel out in IR safe observables (like cross sections), but they leave logarithmic terms depending on scales characterizing virtual and real corrections. The logarithmic remnants become very large near the absolute threshold, so they are important in processes of heavy-particles production. In the absolute threshold limit, the characteristic velocity of the outgoing partons $\beta$ is very small, which means that total energy $\sqrt{\hat{s}}$ of partons in the centre-of-mass system is very close to $m_{\mathrm{th}}$, where $m_{\mathrm{th}}$ is the sum of masses of products in the process. The characteristic scale of the real corrections, that come from the collinear gluon radiation is $m_{\mathrm{th}}\beta^2$, and the characteristic scale of the virtual corrections is proportional to $m_{\mathrm{th}}$. The combined real and virtual corrections give a leading contribution to cross section proportional to $\alpha_{\mathrm{s}} \log^2 \beta^2$. Such logarithms appear in every order of perturbative expansion contributing with $\left(\alpha_{\mathrm{s}} \log^2 \beta^2\right)^n$ in the leading logarithmic (LL) approximation, $\alpha_{\mathrm{s}}^n \log^{2n-1} \beta^2$ in the next-to-leading logarithmic (NLL) approximation, and so on. When $\beta \ll 1$, $\alpha_{\mathrm{s}} \log^2 \beta^2$ may be close or grater than one, and one needs to resum those corrections to all orders. The remnant logarithms are reordered in a new perturbative expansion due to the resummation procedure. The resummation formalism is described in [7, 8]. The fundamental object used in the resummation procedure is the soft anomalous dimension matrix.

The soft-gluon resummation technique that employs the SAD matrices have numerous applications in modern particle physics, in particular in estimates of superparticles hadroproduction. The SAD matrices carry information about colour flow between particles in the studied processes. The soft-gluon resummation effects become very important in cross sections near the threshold for heavy-particles production.

The SAD matrices were calculated for various types of processes. Firstly, calculations were performed for the Drell–Yan processes $2 \to 1$ with two incoming coloured particles and one colour-neutral [9, 10]. Then, there were considered processes $2 \to 2$, such as $q\bar{q} \to q\bar{q}$ and $gg \to q\bar{q}$ for massless and massive products in the final state, in one-loop approximation [8]. This approach was extended to all reactions containing light quarks and gluons [11]. It allowed to obtain predictions for cross sections for production of heavy quarks (especially for the top quark) [12–19], and compare with experimental data. The SAD matrices also play an important role in predictions for squarks and gluinos hadroproduction cross sections. Soft anomalous dimension matrices were calculated at one loop [20–22] and two loops [23–25] for such processes. Recently, a lot of effort has been made to obtain accu-

rate predictions for reactions involving the Higgs boson. Firstly, there was obtained the hadroproduction cross section improved by the soft-gluon resummation at the NNLL approximation [26] and then at the N$^3$LL level [27] for the $2 \to 1$ process: $gg \to H^0$. For the supersymmetric charged Higgs boson hadroproduction, the soft-gluon resummation was performed at two loops for the $bg \to tH^-$ process [28]. Next, the soft-gluon resummation was extended to a new class of processes: $2 \to 3$ containing 4 coloured and 1 colour neutral particles, which gives more accurate predictions for the Higgs boson hadroproduction cross section in association with the top and antitop quarks [1–4].

In this paper, the SAD matrices are derived for $2 \to 3$ processes with 5 coloured particles at one loop in the perturbation theory, $q\bar{q} \to Q\bar{Q}g$ and $gg \to Q\bar{Q}g$. The quark and antiquark in the final state are both massive. Earlier calculations of the SAD matrices in similar reactions have been performed by Sjödahl [5, 6], but only for massless final-state partons. Recently, there have been done parallel calculations for the $q\bar{q} \to Q\bar{Q}g$ channel with massive outgoing particles by Schäfer in [29].

## 2. General formalism

In this paper, we consider the following scattering processes:

$$q^{\alpha}(p_1)\bar{q}^{\beta}(p_2) \to Q^{\gamma}(p_3)\bar{Q}^{\delta}(p_4)g^{a}(p_5) \tag{1}$$

and

$$g^{a}(p_1)g^{b}(p_2) \to Q^{\alpha}(p_3)\bar{Q}^{\beta}(p_4)g^{c}(p_5)\,, \tag{2}$$

where $\alpha$, $\beta$, $\gamma$, $\delta$, $a$, $b$ and $c$ stand for colour indices (Greek letters are used for description of a fundamental representation of SU($N_c$) and Roman letters for an adjoint representation) and $p_i$, $i = 1, \ldots, 5$ denote the momenta of particles. The illustration of an arbitrary $2 \to 3$ process is presented in figure 1.

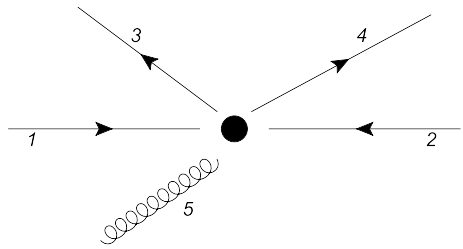


Fig. 1. An example of a particle collision in a $2 \to 3$ process.

It follows from factorization theorems in QCD that the multi-jet hadroproduction amplitudes may be factorized into hard and soft parts, see *e.g.* [8, 11]. The soft function $S_{IJ}$ fulfills the renormalization group equation

$$\left(\mu\frac{\partial}{\partial\mu}+\beta(g)\frac{\partial}{\partial g}\right)S_{IJ}=-\left(\Gamma_{\mathrm{S}}^{\prime\dagger}\right)_{IB}S_{BJ}-S_{IA}\left(\Gamma_{\mathrm{S}}\right)_{AJ}\,, \tag{3}$$

where $S_{IJ}$ is a matrix in colour space and carries information about soft wide angle gluon emissions, indices $I$, $J$ correspond to colour tensors constructed from $\mathrm{SU}(N_{\mathrm{c}})$ representations. They depend on a studied process: the colour charges of participating particles and the exchange channel. For example, if we consider a quark–antiquark annihilitation, $I$ and $J$ tensors correspond to a flow of a colour singlet or octet in the $s$-channel. At one loop, the soft anomalous dimension matrix is defined as follows [8, 11]:

$$\Gamma_{\mathrm{S}}^{\prime}\left(g\right)=-\frac{g}{2}\frac{\partial}{\partial g}\mathrm{Res}_{\epsilon\to0}Z_{\mathrm{S}}\left(g,\epsilon\right)\,, \tag{4}$$

where $g$ is the coupling constant for QCD, $Z_{\mathrm{S}}\left(g,\epsilon\right)$ — a renormalization matrix of the soft matrix $S_{IJ}$. $Z_{\mathrm{S}}$ receives contributions from the soft gluons. The general form of the SAD matrix can be obtained from Refs. [30–32]. However, in our explicit calculations, we apply the method elaborated in [8, 11].

To get $Z_{\mathrm{S}}$, one needs to sum over the contributions $Z_{\mathrm{S}}^{(D)}$ of relevant Feynman diagrams. Each contribution $Z_{\mathrm{S}}^{(D)}$ to $Z_{\mathrm{S}}$ coming from a single Feynman diagram $D$ can be factorized into a colour factor and a kinematic factor

$$Z_{\mathrm{S}}^{(D)}\propto\text{colour factor}\times\text{kinematic factor}\,. \tag{5}$$

The colour part of every diagram is represented by $\mathrm{SU}(N_{\mathrm{c}})$ tensors decomposed in an orthogonal and normalized basis. The vectors from colour basis are connected with a soft-gluon line which is represented by colour tensor $if_{abc}$. The form of $Z_{\mathrm{S}}$ depends on whether the partons between which there is an exchange of the soft gluon are massive or massless (see figure 2). For massive particles $i$ and $j$ [8, 11],

$$Z_{\mathrm{S}}^{(D)}\left(g,\epsilon\right)=c^{ij}s_{ij}\frac{\alpha}{\pi}\frac{1}{\epsilon}\left(L_{\beta}^{(ij)}+L_{i}+L_{j}-1\right)\,. \tag{6}$$

For a massive particle $i$ and a massless particle $j$,

$$Z_{\mathrm{S}}^{(D)}\left(g,\epsilon\right)=-c^{ij}s_{ij}\frac{\alpha}{2\pi}\frac{1}{\epsilon}\left(\ln\left[\frac{v_{ij}^{2}s}{2m_{i}^{2}}\right]-L_{i}-\ln\nu_{j}+1\right)\,. \tag{7}$$

For massless particles $i$ and $j$,

$$Z_{\mathrm{S}}^{(D)}(g,\epsilon) = -c^{ij} s_{ij} \frac{\alpha}{\pi} \frac{1}{\epsilon} \left( \ln \left[ \frac{\delta_i \delta_j v_i \cdot v_j}{2} \right] - \frac{1}{2} \ln (\nu_i \nu_j) + 1 \right) . \tag{8}$$

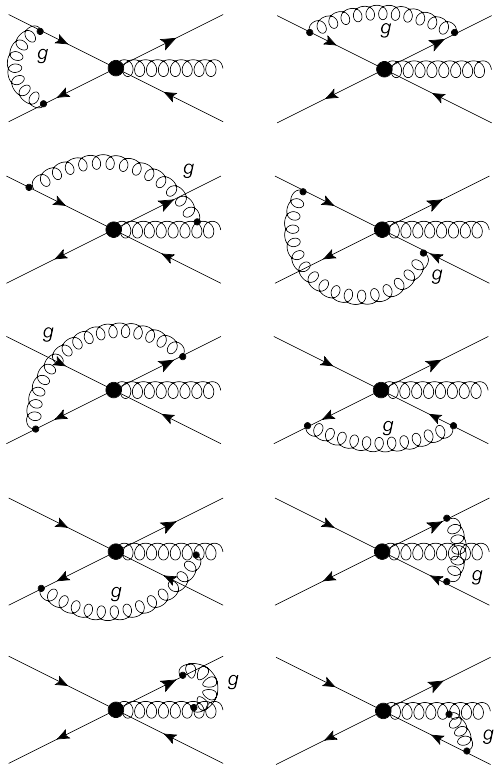


Fig. 2. Feynman diagrams contributing to $Z_{\mathrm{S}}$ for process $q\bar{q} \to Q\bar{Q}g$ (for $gg \to Q\bar{Q}g$, the topologies are analogous). The soft gluon is indicated by $g$ in the diagrams, and it is exchanged between external lines that are approximated as Wilson lines. The coupling of the soft gluon to the Wilson lines is eikonal, see *e.g.* [8].

In the above equations, factors $c^{ij}$ stand for colour factors, the number $s_{ij}$ is related to the type of particles and the direction of the momentum flow in a diagram. Namely,

$$s_{ij} = \Delta_i \Delta_j \delta_i \delta_j \, . \tag{9}$$

The factors $\Delta_i$ depend on the type of particles between which the exchange of the gluon occurs, they have values: $+1(-1)$ for a quark (antiquark). The factors $\delta_i = +1(-1)$ for the same (opposite) direction of momentum flow between a parton and the soft gluon. Vectors $v_i$ are rescaled momenta of the

particles $v_i^\mu = \frac{p_i^\mu}{Q}$, where $Q = \sqrt{\frac{\hat{s}}{2}}$, and $v_{ij} = v_i \cdot v_j$. The factors $\nu_i = \frac{(v_i \cdot n)^2}{|n|^2}$ depend on a choice of the reference vector $n^\mu$ of the axial gauge. In the axial gauge $A^0 = 0$ in the center-of-mass system of the colliding partons, one has $\nu_i = \frac{1}{2}$. The function $L_\beta^{(ij)}$ depends on the relative velocity $\beta_{ij}$ of the outgoing partons

$$L_\beta^{(ij)} = \frac{1 - 2m^2/\hat{s}_{ij}}{\beta_{ij}} \left( \ln \frac{1 - \beta_{ij}}{1 + \beta_{ij}} + i\pi \right), \tag{10}$$

where $\beta_{ij} = \sqrt{1 - 4m^2/\hat{s}_{ij}}$ and $\hat{s}_{ij} = (p_i + p_j)^2$. In the processes considered, the massive particles are labelled 3 and 4, hence in what follows, $\beta_{34}$ will be used. $L_i$ are dependent on the choice of gauge: $L_i = \frac{1}{2}\left[L_i(+n) + L_i(-n)\right]$, where

$$\begin{aligned} L_i(\pm n) \;=\; & \frac{1}{2} \frac{|v_i \cdot n|}{\sqrt{(v_i \cdot n)^2 - 2m^2 n^2/s}} \\ & \times \left[ \ln \left( \frac{\delta(\pm n)\, 2m^2/s - |v_i \cdot n| - \sqrt{(v_i \cdot n)^2 - 2m^2 n^2/s}}{\delta(\pm n)\, 2m^2/s - |v_i \cdot n| + \sqrt{(v_i \cdot n)^2 - 2m^2 n^2/s}} \right) \right. \\ & \left. + \ln \left( \frac{\delta(\pm n)\, n^2 - |v_i \cdot n| - \sqrt{(v_i \cdot n)^2 - 2m^2 n^2/s}}{\delta(\pm n)\, n^2 - |v_i \cdot n| + \sqrt{(v_i \cdot n)^2 - 2m^2 n^2/s}} \right) \right]. \end{aligned} \tag{11}$$

Contributions $L_i$ also appear in the self-interaction terms for the heavy quarks (antiquarks). The contribution from the self-interaction of heavy quarks (antiquarks) is

$$\frac{\alpha_\mathrm{s}}{\pi} T_R \frac{N_\mathrm{c}^2 - 1}{N_\mathrm{c}} \left( L_i + L_j - 2 \right) \mathbf{1}, \tag{12}$$

where $\mathbf{1}$ is the identity matrix in the colour space and the factor $T_R$ comes from the normalization of generators and equals $\frac{1}{2}$. The contribution from the self-interaction of heavy quarks (antiquarks) is added to the soft anomalous dimension matrix and the dependence of $\Gamma_\mathrm{S}'$ on $L_i$ is cancelled out. Following Refs. [8, 11], the Drell–Yan contribution is subtracted from the soft anomalous dimension matrix. At one loop, the Drell–Yan SAD matrix takes the form of $\frac{\alpha_\mathrm{s}}{\pi} C_F \mathbf{1}$ ($\frac{\alpha_\mathrm{s}}{\pi} C_A \mathbf{1}$) for the partons in the colour triplet (octet) state and $C_A = T_R 2N_\mathrm{c}$ and $C_F = T_R \frac{N_\mathrm{c}^2 - 1}{N_\mathrm{c}}$. The final form of the soft anomalous dimension matrix $\Gamma_\mathrm{S}(g, \epsilon)$ is the following:

$$\Gamma_\mathrm{S}(g, \epsilon) = \Gamma_\mathrm{S}'(g, \epsilon) + \frac{\alpha_\mathrm{s}}{\pi} T_R \frac{N_\mathrm{c}^2 - 1}{N_\mathrm{c}} \left( L_3 + L_4 - 2 \right) \mathbf{1} - \frac{1}{2} \sum_i C_{A,F}^i \mathbf{1}, \tag{13}$$

where $i$ — all massless particles in the examined process.

In this paper, processes with five interacting particles are considered (see figure 1).

To fully describe the phase space of such a physical system, one needs five independent variables: the global azimuthal angle $\phi$, which carries information about the rotation symmetry of the reaction and four Mandelstam-type variables:

$$\begin{aligned} t_1 &= (p_3 - p_1)^2 \,, \\ t_2 &= (p_4 - p_2)^2 \,, \\ u_1 &= (p_3 - p_2)^2 \,, \\ u_2 &= (p_4 - p_1)^2 \,. \end{aligned} \tag{14}$$

The remaining scalar products of particle momenta $p_i \cdot p_5$ $(i = 1, 2, 3, 4)$ may be expressed in terms of above variables:

$$\begin{aligned} p_1 \cdot p_5 &= \tfrac{1}{2}\left(t_1 + u_2 + s - m_3^2 - m_4^2\right) \,, \\ p_2 \cdot p_5 &= \tfrac{1}{2}\left(t_2 + u_1 + s - m_3^2 - m_4^2\right) \,, \\ p_3 \cdot p_5 &= \tfrac{1}{2}\left(t_2 + u_2 + s - m_3^2 - m_4^2\right) \,, \\ p_4 \cdot p_5 &= \tfrac{1}{2}\left(t_1 + u_1 + s - m_3^2 - m_4^2\right) \,, \end{aligned} \tag{15}$$

where $m_{3,4}$ is the mass of heavy quark (antiquark).

## 3. Results

In this section, we collect results for the soft anomalous dimension matrices for two processes $q\bar{q} \to Q\bar{Q}g$ and $gg \to Q\bar{Q}g$, where $q$, $\bar{q}$ denote the massless quark/antiquark, and $Q$, $\bar{Q}$ — the massive quark/antiquark. Calculations of the colour factors were obtained in the $s$-channel basis, using the package ColorMath [6] for Mathematica. The colour factors were combined with formulas (4), (6)–(8), also (13), and $\Gamma_S$ was obtained. It is convenient to introduce new variables $\Lambda$, $\Omega$, $\Gamma$, $\Sigma$, which are defined in the following way:

$$\begin{aligned} \Lambda &= T_1 + T_2 + U_1 + U_2 \,, \\ \Omega &= T_1 + T_2 - U_1 - U_2 \,, \\ \Gamma &= T_1 - T_2 + U_1 - U_2 \,, \\ \Sigma &= T_1 - T_2 - U_1 + U_2 \,, \end{aligned} \tag{16}$$

where

$$
\begin{aligned}
T_1 &= \ln\left(\frac{2p_1\cdot p_3}{m_3\sqrt{s}}\right)-\frac{1-i\pi}{2}\,,\\
T_2 &= \ln\left(\frac{2p_2\cdot p_4}{m_4\sqrt{s}}\right)-\frac{1-i\pi}{2}\,,\\
U_1 &= \ln\left(\frac{2p_2\cdot p_3}{m_4\sqrt{s}}\right)-\frac{1-i\pi}{2}\,,\\
U_2 &= \ln\left(\frac{2p_1\cdot p_4}{m_3\sqrt{s}}\right)-\frac{1-i\pi}{2}\,.
\end{aligned}
\tag{17}
$$

In this study, the case is considered of the mass of quark and antiquark that have the same value $m = m_3 = m_4$; we prefer to keep the more general definition of the kinematic factors keeping in mind possibility to apply formalism to general case of $2 \to 3$ process.

In what follows, the SAD matrices will be presented in terms of the independent variables $\Lambda$, $\Omega$, $\Gamma$, $\Sigma$ and the variables $v_{i5} = 2p_i \cdot p_5/s$ that can be expressed by $\Lambda$, $\Omega$, $\Gamma$, $\Sigma$ with equalities (11), (12) and (13). The variables $v_{i5}$ are kept in order to simplify the form of the matrices.

### *3.1.* $q\bar{q} \to Q\bar{Q}g$

The following orthogonal and normalized colour basis was used in the calculations [5]:

$$
\begin{aligned}
T^1_{\alpha\beta\gamma\zeta a} &= \frac{1}{\sqrt{N_{\rm c}\left(N_{\rm c}^2-1\right)T_R}}\delta_{\alpha\beta}t^a_{\gamma\zeta}\,,\\
T^2_{\alpha\beta\gamma\zeta a} &= \frac{1}{\sqrt{N_{\rm c}\left(N_{\rm c}^2-1\right)T_R}}\delta_{\gamma\zeta}t^a_{\beta\alpha}\,,\\
T^3_{\alpha\beta\gamma\zeta a} &= \frac{1}{\sqrt{2N_{\rm c}\left(N_{\rm c}^2-1\right)\left(T_R\right)^3}}t^b_{\beta\alpha}t^c_{\gamma\zeta}if_{bca}\,,\\
T^4_{\alpha\beta\gamma\zeta a} &= \frac{\sqrt{N_{\rm c}}}{\sqrt{2\left(N_{\rm c}^2-4\right)\left(N_{\rm c}^2-1\right)\left(T_R\right)^3}}t^b_{\beta\alpha}t^c_{\gamma\zeta}d_{bca}\,.
\end{aligned}
\tag{18}
$$

Notice that indices of the adjoint representation are $a$, $b$, $c$ and indices of the fundamental representation are $\alpha$, $\beta$, $\gamma$ and $\zeta$. The following results are valid for $N_{\rm c} \geq 3$ [5].

The soft anomalous dimension matrix $\Gamma_{q\bar{q}\to Q\bar{Q}g}$ can be split into two parts

$$
\Gamma_{q\bar{q}\to Q\bar{Q}g} = \Gamma^{(1)}_{q\bar{q}\to Q\bar{Q}g}\left(\Lambda,\Omega,\Gamma,\Sigma\right) + \Gamma^{(2)}_{q\bar{q}\to Q\bar{Q}g}\left(v_{i5}\right)\,,
\tag{19}
$$

where $\Gamma^{(1)}$ receives contributions from the soft gluon exchanges between particles $1, 2, 3, 4$, and $\Gamma^{(2)}$ from exchanges between particles $i$ and $5$, with $i = 1, 2, 3, 4$. Hence,

$$\Gamma^{(1)}_{q\bar{q}\to Q\bar{Q}g} = \frac{\alpha_s}{\pi} T_R \times \begin{pmatrix} \frac{1+\left(1-N_c^2\right)L_\beta}{N_c} & \frac{\Omega}{N_c} & \frac{\sqrt{N_c^2-4}}{\sqrt{2}N_c}\Omega & \frac{\Gamma}{\sqrt{2}} \\ \frac{\Omega}{N_c} & \frac{2+2L_\beta+N_c^2}{2N_c} & \frac{\sqrt{N_c^2-4}}{\sqrt{2}N_c}\Omega & \frac{\Sigma}{\sqrt{2}} \\ \frac{\sqrt{N_c^2-4}}{\sqrt{2}N_c}\Omega & \frac{\sqrt{N_c^2-4}}{\sqrt{2}N_c}\Omega & \frac{4+4L_\beta+\left(N_c^2-12\right)\Omega+N_c^2(2+\Lambda)}{4N_c} & \frac{1}{4}\sqrt{N_c^2-4}(\Gamma+\Sigma) \\ \frac{\Gamma}{\sqrt{2}} & \frac{\Sigma}{\sqrt{2}} & \frac{1}{4}\sqrt{N_c^2-4}(\Gamma+\Sigma) & \frac{4+4L_\beta+\left(N_c^2-4\right)\Omega+N_c^2(2+\Lambda)}{4N_c} \end{pmatrix}, \tag{20}$$

and

$$\Gamma^{(2)}_{q\bar{q}\to Q\bar{Q}g} = \frac{\alpha_s}{\pi} T_R \times \begin{pmatrix} N_c \ln(v_{15}v_{25}) & 0 & 0 & \frac{1}{\sqrt{2}}\ln\left(\frac{v_{45}}{v_{35}}\right) \\ 0 & \frac{1}{2}N_c\ln(v_{35}v_{45}) & 0 & \ln\left(\frac{v_{25}}{v_{15}}\right)\sqrt{2} \\ 0 & 0 & \frac{1}{4}N_c\ln\left(v_{15}^2v_{25}^2v_{35}v_{45}\right) & \frac{1}{4}\ln\left(\frac{v_{25}^2v_{45}}{v_{15}^2v_{35}}\right)\sqrt{N_c^2-4} \\ \frac{1}{\sqrt{2}}\ln\left(\frac{v_{45}}{v_{35}}\right) & \ln\left(\frac{v_{25}}{v_{15}}\right)\sqrt{2} & \frac{1}{4}\ln\left(\frac{v_{25}^2v_{45}}{v_{15}^2v_{35}}\right)\sqrt{N_c^2-4} & \frac{1}{4}N_c\ln\left(v_{15}^2v_{25}^2v_{35}v_{45}\right) \end{pmatrix}$$

$$+\frac{\alpha_s}{\pi} T_R \times \mathbf{diag}\left(\frac{i\pi}{N_c}, i\pi\frac{1-N_c^2}{N_c}, i\pi\frac{2-N_c^2}{2N_c}, i\pi\frac{2-N_c^2}{2N_c}\right). \tag{21}$$

The SAD matrices for $q\bar{q} \to Q\bar{Q}g$ were calculated in parallel in [29]. Note that the obtained SAD matrix is complex symmetric. This property has been proved to hold in general in an orthonormal basis [33]. The same feature will be found also for the $gg$-channel. For clarity, we denoted $L_\beta^{(34)}$ as $L_\beta$ in all the matrices. The general form of the soft anomalous dimension matrix is rather complicated, hence, in order to provide more insight into its properties, we consider special kinematical configurations for which the matrix simplifies. First, we consider the case when the momenta of the outgoing quark and antiquark are equal, $p_3^\mu = p_4^\mu$. Then variables $\Lambda$, $\Omega$, $\Gamma$, $\Sigma$ reduce to $\Lambda \to \Lambda' = 2T_1 + 2U_1$, $\Sigma \to \Sigma' = 2T_1 - 2U_1$, $\Gamma \to 0$, $\Omega \to 0$. In this special case, it is convenient to introduce a variable $\beta = \sqrt{1 - \frac{4m^2}{\hat{s}}}$. In this limit, the form of the soft anomalous matrix becomes significantly simpler

$$\Gamma^{(1)}_{q\bar{q}\to Q\bar{Q}g}\left(p_3^\mu = p_4^\mu\right) = \frac{\alpha_{\rm s}}{\pi} T_R$$
$$\times \begin{pmatrix} \frac{1+\left(1-N_{\rm c}^2\right)L_\beta}{N_{\rm c}} & 0 & 0 & 0 \\ 0 & \frac{2+2L_\beta+N_{\rm c}^2}{2N_{\rm c}} & 0 & \frac{\Sigma'}{\sqrt{2}} \\ 0 & 0 & \frac{4+4L_\beta+N_{\rm c}^2(2+\Lambda')}{4N_{\rm c}} & \frac{\Sigma'}{4}\sqrt{N_{\rm c}^2-4} \\ 0 & \frac{\Sigma'}{\sqrt{2}} & \frac{\Sigma'}{4}\sqrt{N_{\rm c}^2-4} & \frac{4+4L_\beta+N_{\rm c}^2(2+\Lambda')}{4N_{\rm c}} \end{pmatrix}, \tag{22}$$

$$\Gamma^{(2)}_{q\bar{q}\to Q\bar{Q}g}\left(p_3^\mu = p_4^\mu\right) = \frac{\alpha_{\rm s}}{\pi} T_R$$
$$\times \begin{pmatrix} N_{\rm c}\ln(v_{15}v_{25}) & 0 & 0 & 0 \\ 0 & N_{\rm c}\ln v_{35} & 0 & \ln\left(\frac{v_{25}}{v_{15}}\right)\sqrt{2} \\ 0 & 0 & \frac{1}{2}N_{\rm c}\ln(v_{15}v_{25}v_{35}) & \frac{1}{2}\ln\left(\frac{v_{25}}{v_{15}}\right)\sqrt{N_{\rm c}^2-4} \\ 0 & \ln\left(\frac{v_{25}}{v_{15}}\right)\sqrt{2} & \frac{1}{2}\ln\left(\frac{v_{25}}{v_{15}}\right)\sqrt{N_{\rm c}^2-4} & \frac{1}{2}N_{\rm c}\ln(v_{15}v_{25}v_{35}) \end{pmatrix}$$
$$+\frac{\alpha_{\rm s}}{\pi} T_R \times \mathbf{diag}\left(\frac{i\pi}{N_{\rm c}},\, i\pi\frac{1-N_{\rm c}^2}{N_{\rm c}},\, i\pi\frac{2-N_{\rm c}^2}{2N_{\rm c}},\, i\pi\frac{2-N_{\rm c}^2}{2N_{\rm c}}\right). \tag{23}$$

It can be seen that the soft anomalous dimension matrix can be divided into two blocks: $\mathbf{1}\times\mathbf{1}$ and $\mathbf{3}\times\mathbf{3}$.

Next, the limit $\Sigma' = 0$ is performed that corresponds to $p_1\cdot p_3 = p_2\cdot p_3$. The obtained matrix has a diagonal form

$$\Gamma_{q\bar{q}\to Q\bar{Q}g}\left(\Sigma'=0\right) = \frac{\alpha_{\rm s}}{\pi} T_R \times \left\{ \frac{1}{N_{\rm c}} \times \mathbf{diag}\left(1+\left(1-N_{\rm c}^2\right)L_\beta,\, 1+L_\beta+\frac{N_{\rm c}^2}{2},\right.\right.$$
$$1+L_\beta+\frac{N_{\rm c}^2}{4}\left(2+\Lambda'\right), 1+L_\beta+\frac{N_{\rm c}^2}{4}\left(2+\Lambda'\right)\Big)$$
$$+\mathbf{diag}\left(2N_{\rm c}\ln v_{15},\, N_{\rm c}\ln v_{35},\, \frac{1}{2}N_{\rm c}\ln\left(v_{15}^2 v_{35}\right),\, \frac{1}{2}N_{\rm c}\ln\left(v_{15}^2 v_{35}\right)\right)$$
$$\left.+\mathbf{diag}\left(\frac{i\pi}{N_{\rm c}},\, i\pi\frac{1-N_{\rm c}^2}{N_{\rm c}},\, i\pi\frac{2-N_{\rm c}^2}{2N_{\rm c}},\, i\pi\frac{2-N_{\rm c}^2}{2N_{\rm c}}\right)\right\}. \tag{24}$$

#### 3.1.1. Analysis of the eigenvalues for $q\bar{q}\to Q\bar{Q}g$

In this section, we consider the behaviour of the SAD eigenvalues for $p_3 = p_4$ and two different scattering angles $\theta$ (90° and 30°), where $\theta$ is

an angle between the incoming and outgoing partons in the CMS frame. $\theta = 90^\circ$ represents the most symmetric case, and the choice of $\theta = 30^\circ$ represents a less symmetric configuration. The limit $\Sigma' \to 0$ corresponds to the case of $\theta = 90^\circ$. This analysis must be done carefully because $L_\beta^{(34)}$ in the limit of $\beta_{34} \to 0$ gives singular terms $\propto \frac{i}{\beta_{34}}$. We need to execute three steps. While performing the limit of $\beta_{34} \to 0$, one subtracts the singular terms from the SAD matrix and then the limit of $\beta \to 0$ may be studied. Finally, we present results after a subtraction of the asymptotic small-$\beta$ behaviour that is treated analytically. Numerical calculations were performed for the $N_c = 3$ case. The eigenvalues of $\tilde{\Gamma}_S$ do not contain the prefactor $\frac{\alpha_s}{\pi}$. The relation between the full SAD matrix $\Gamma_S$ and $\tilde{\Gamma}_S$ is $\Gamma_S = \frac{\alpha_s}{\pi}\tilde{\Gamma}_S$. The singular matrix subtracted from $\tilde{\Gamma}_S$ has a form of $\frac{i\pi}{\beta_{34}} \times \mathbf{diag}\left(-\frac{2}{3}, \frac{1}{12}, \frac{1}{12}, \frac{1}{12}\right)$. The singular matrix comes from the exchange of the soft gluon between massive outgoing quark and antiquark. Hence, this matrix contains Coulomb corrections, see *e.g.* [21] and references therein.

For a general $\beta$, there is a degeneracy of eigenvalues for $\theta = 90^\circ$, there are three different eigenvalues. For $\theta = 30^\circ$, there is no degeneracy. All eigenvalues are complex with non-trival real and imaginary part. For $\theta = 90^\circ$, there are two different values of the imaginary part of eigenvalues instead of four, which is the case of $30^\circ$.

For $\beta \to 0$, one finds a singular term proportional to $\log\beta$ which gives a contribution to the real part of the eigenvalues. Each eigenvalue of $\Gamma_S$ has the same leading behaviour in $\beta \to 0$ for both scattering angles. One finds single asymptotic form of the eigenvalues of small $\beta$:

$$\lambda^{\text{sing}} = 6\log\beta\,. \tag{25}$$

In figures 3 and 4, we show regularized eigenvalues. They are defined as $\lambda_i^{\text{reg}} = \lambda_i - \lambda^{\text{sing}}$. One observes a quite similar behaviour of the regularized eigensystem for $\theta = 90^\circ$ and $\theta = 30^\circ$. In figure 3, one can see that all $\text{Re}(\lambda^{\text{reg},90^\circ})$ are either constant ($\lambda_1$) or slightly increasing ($\lambda_2$,$\lambda_{3,4}$) up to $\beta \approx 0.4$. $\text{Im}(\lambda^{90^\circ})$ is constant in $\beta$. In the case of $\theta = 30^\circ$, the real and imaginary part of $\lambda_1$ shows a constant behaviour. The real parts of $\lambda_2$, $\lambda_3$ and $\lambda_4$ exhibit a similar behaviour for small $\beta$ — they are slowly varying for moderate $\beta$, then for $\beta > 0.6$, they are rapidly increasing. The imaginary parts of these remaining eigenvalues are nearly constant for $\beta < 0.7$, and then start to slowly decrease ($\lambda_2$ and $\lambda_3$) or slowly increase ($\lambda_4$).

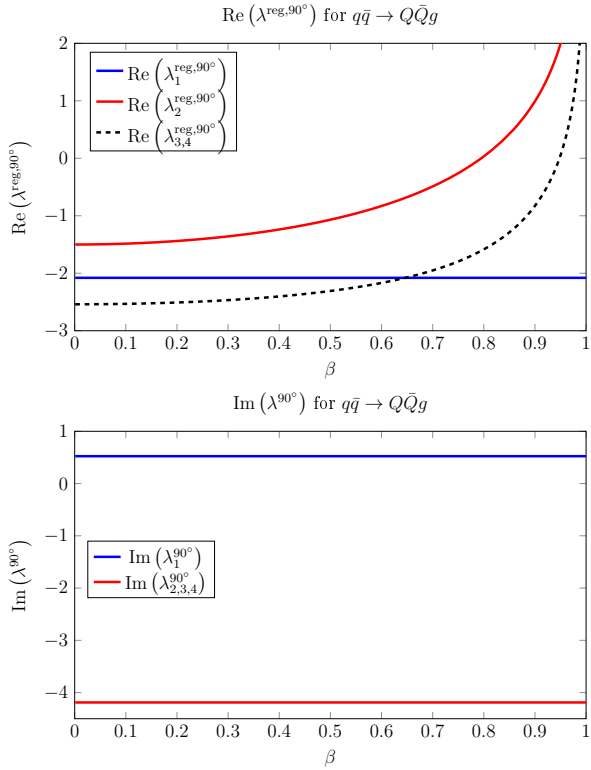


Fig. 3. The real (top) and imaginary (bottom) parts of the eigenvalues of $\tilde{\Gamma}_{\mathrm{S}}$ for $q\bar{q} \to Q\bar{Q}g$ at $\theta = 90^\circ$.

### *3.2.* $gg \to Q\bar{Q}g$

The following orthogonal and normalized colour basis was used in the calculations [5]:

$$
\begin{aligned}
T^1_{ab\alpha\beta c} &= \frac{1}{(N_{\mathrm{c}}^2-1)\sqrt{T_R}} t^c_{\alpha\beta}\delta_{ab}\,,\\
T^2_{ab\alpha\beta c} &= \frac{1}{N_{\mathrm{c}}\sqrt{2\,(N_{\mathrm{c}}^2-1)\,T_R}} i f_{abc}\delta_{\alpha\beta}\,,\\
T^3_{ab\alpha\beta c} &= \frac{1}{\sqrt{2\,(N_{\mathrm{c}}^2-4)\,(N_{\mathrm{c}}^2-1)\,T_R}} d_{abc}\delta_{\alpha\beta}\,,\\
T^4_{ab\alpha\beta c} &= \frac{1}{2N_{\mathrm{c}}\sqrt{(N_{\mathrm{c}}^2-1)\,(T_R)^3}} i f_{abn} i f_{mcn} t^m_{\alpha\beta}\,,\\
T^5_{ab\alpha\beta c} &= \frac{1}{\sqrt{4\,(N_{\mathrm{c}}^2-4)\,(N_{\mathrm{c}}^2-1)\,(T_R)^3}} d_{abn} i f_{mcn} t^m_{\alpha\beta}\,,
\end{aligned}
$$

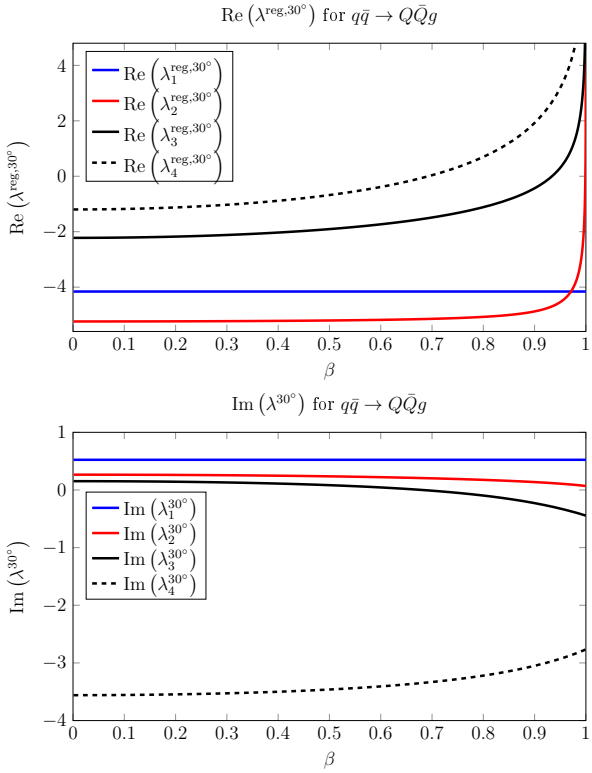


Fig. 4. The real (top) and imaginary (bottom) parts of the eigenvalues of $\tilde{\Gamma}_{\mathrm{S}}$ for $q\bar{q} \to Q\bar{Q}g$ at $\theta = 30^\circ$.

$$
\begin{aligned}
T^6_{ab\alpha\beta c} &= \frac{1}{\sqrt{4\left(N_{\mathrm{c}}^2-4\right)\left(N_{\mathrm{c}}^2-1\right)\left(T_R\right)^3}} i f_{abn} d_{mcn} t^m_{\alpha\beta}\,, \\
T^7_{ab\alpha\beta c} &= \frac{1}{\sqrt{4\left(N_{\mathrm{c}}^2-4\right)^2\left(N_{\mathrm{c}}^2-1\right)\left(T_R\right)^3}} d_{abn} d_{mcn} t^m_{\alpha\beta}\,, \\
T^8_{ab\alpha\beta c} &= \frac{1}{\sqrt{2\left(N_{\mathrm{c}}^2-4\right)\left(N_{\mathrm{c}}^2-1\right)\left(T_R\right)^3}} P^{10+\bar{10}}_{abmc} t^m_{\alpha\beta}\,, \\
T^9_{ab\alpha\beta c} &= \frac{1}{\sqrt{2\left(N_{\mathrm{c}}^2-4\right)\left(N_{\mathrm{c}}^2-1\right)\left(T_R\right)^3}} P^{10-\bar{10}}_{abmc} t^m_{\alpha\beta}\,, \\
T^{10}_{ab\alpha\beta c} &= \frac{-1}{\sqrt{N_{\mathrm{c}}^2\left(N_{\mathrm{c}}+3\right)\left(N_{\mathrm{c}}-1\right)\left(T_R\right)^3}} P^{27}_{abmc} t^m_{\alpha\beta}\,, \\
T^{11}_{ab\alpha\beta c} &= \frac{1}{\sqrt{N_{\mathrm{c}}^2\left(N_{\mathrm{c}}-3\right)\left(N_{\mathrm{c}}+1\right)\left(T_R\right)^3}} P^{0}_{abmc} t^m_{\alpha\beta}\,,
\end{aligned}
\tag{26}
$$

where

$$
\begin{aligned}
P^{10+\bar{1}0}_{abcd} &= \frac{1}{2}\left(\delta_{ac}\delta_{bd}-\delta_{ad}\delta_{cb}\right)-\frac{1}{N_{\rm c}}f_{abg}f_{cdg}\,,\\
P^{10-\bar{1}0}_{abcd} &= \frac{1}{2}d_{acg}if_{bgd}-\frac{1}{2}d_{bgd}if_{acg}\,,\\
P^{27}_{abcd} &= \frac{N_{\rm c}}{4\left(N_{\rm c}+2\right)}d_{abg}d_{cdg}+\frac{1}{2}f_{adg}f_{cbg}-\frac{1}{4}f_{abg}f_{cdg}+\frac{1}{4}\delta_{ad}\delta_{bc}+\frac{1}{4}\delta_{ac}\delta_{bd}\\
&\quad+\frac{1}{2\left(N_{\rm c}+1\right)}\delta_{ab}\delta_{cd}\,,\\
P^{0}_{abcd} &= -\frac{N_{\rm c}}{4\left(N_{\rm c}+2\right)}d_{abg}d_{cdg}-\frac{1}{2}f_{adg}f_{cbg}+\frac{1}{4}f_{abg}f_{cdg}+\frac{1}{4}\delta_{ad}\delta_{bc}+\frac{1}{4}\delta_{ac}\delta_{bd}\\
&\quad-\frac{1}{2\left(N_{\rm c}+1\right)}\delta_{ab}\delta_{cd}\,. \qquad (27)
\end{aligned}
$$

As for the $q\bar{q}\to Q\bar{Q}g$ case, the soft anomalous dimension matrix $\Gamma_{gg\to Q\bar{Q}g}$ is split into two parts

$$
\Gamma_{gg\to Q\bar{Q}g}=\Gamma^{(1)}_{gg\to Q\bar{Q}g}\left(\Lambda,\Omega,\Gamma,\Sigma\right)+\Gamma^{(2)}_{gg\to Q\bar{Q}g}\left(v_{i5}\right)\,, \qquad (28)
$$

where

$$\Gamma^{(1)}_{gg\to Q\bar{Q}g} = \frac{\alpha_s}{\pi} T_R$$

$$\times \begin{pmatrix}
\frac{1+\left(1-N_c^2\right)L_\beta}{N_c} & -\Omega & 0 & -\frac{\Omega}{\sqrt{2}} & \frac{\Gamma}{\sqrt{2}} & 0 & \dots \\
-\Omega & \frac{2+2L_\beta+N_c^2(2+\Lambda)}{2N_c} & 0 & 0 & 0 & \frac{\Gamma}{2} & \dots \\
0 & 0 & \frac{1+\left(1-N_c^2\right)L_\beta}{N_c} & 0 & 0 & 0 & \dots \\
-\frac{\Omega}{\sqrt{2}} & 0 & 0 & \frac{4+4L_\beta+N_c^2(2+\Lambda)}{4N_c} & -\frac{\Sigma N_c}{4} & 0 & \dots \\
\frac{\Gamma}{\sqrt{2}} & 0 & 0 & -\frac{\Sigma N_c}{4} & \frac{4+4L_\beta+N_c^2(2+\Lambda)}{4N_c} & -\frac{\Omega}{\sqrt{2}} & \dots \\
0 & \frac{\Gamma}{2} & 0 & 0 & \frac{-\Omega}{\sqrt{2}} & \frac{2+2L_\beta+N_c^2(2+\Lambda)}{2N_c} & \dots \\
0 & \frac{\Omega}{2\sqrt{2}}\sqrt{\frac{(N_c-3)(N_c-1)(N_c+2)}{(N_c-2)}} & -\Omega\sqrt{\frac{N_c-3}{2(N_c-1)}} & \frac{\Omega}{2}\sqrt{\frac{(N_c-3)(N_c+2)}{(N_c-2)(N_c-1)}} & 0 & \frac{\Sigma}{2\sqrt{2}}\sqrt{\frac{(N_c-3)(N_c-1)(N_c+2)}{(N_c-2)}} & \dots \\
0 & -\frac{\Omega\sqrt{2}}{\sqrt{N_c^2-4}} & \frac{-\Omega}{\sqrt{2}} & -\frac{\Omega\left(N_c^2-12\right)}{4\sqrt{N_c^2-4}} & \frac{\Gamma}{4}\sqrt{N_c^2-4} & \frac{N_c\Sigma}{\sqrt{2}\sqrt{N_c^2-4}} & \dots \\
0 & \frac{\Omega}{2\sqrt{2}}\sqrt{\frac{(N_c+3)(N_c+1)(N_c-2)}{(N_c+2)}} & -\Omega\sqrt{\frac{N_c+3}{2(N_c+1)}} & \frac{-\Omega}{2}\sqrt{\frac{(N_c-2)(N_c+3)}{(N_c+1)(N_c+2)}} & 0 & \frac{-\Sigma}{2\sqrt{2}}\sqrt{\frac{(N_c-2)(N_c+1)(N_c+3)}{(N_c+2)}} & \dots \\
0 & 0 & \frac{\Gamma}{\sqrt{2}} & \frac{\Gamma}{4}\sqrt{N_c^2-4} & \frac{-\Omega}{4}\sqrt{N_c^2-4} & 0 & \dots \\
0 & 0 & \frac{-\Omega\sqrt{2}}{\sqrt{N_c^2-1}} & -\Omega\sqrt{\frac{N_c^2-4}{N_c^2-1}} & 0 & 0 & \dots
\end{pmatrix}$$

$$
\begin{pmatrix}
\dots & 0 & 0 & 0 & 0 & 0 \\
\dots & \frac{\Omega}{2\sqrt{2}}\sqrt{\frac{(N_c-3)(N_c-1)(N_c+2)}{(N_c-2)}} & \frac{\Omega\sqrt{2}}{\sqrt{N_c^2-4}} & \frac{\Omega}{2\sqrt{2}}\sqrt{\frac{(N_c+3)(N_c+1)(N_c-2)}{(N_c+2)}} & 0 & 0 \\
\dots & -\Omega\sqrt{\frac{N_c-3}{2(N_c-1)}} & \frac{-\Omega}{\sqrt{2}} & -\Omega\sqrt{\frac{N_c+3}{2(N_c+1)}} & \frac{\Gamma}{\sqrt{2}} & \frac{-\Omega\sqrt{2}}{\sqrt{N_c^2-1}} \\
\dots & \frac{\Omega}{2}\sqrt{\frac{(N_c-3)(N_c+2)}{(N_c-2)(N_c-1)}} & -\frac{\Omega\left(N_c^2-12\right)}{4\sqrt{N_c^2-4}} & -\frac{\Omega}{2}\sqrt{\frac{(N_c+3)(N_c-2)}{(N_c+2)(N_c+1)}} & \frac{\Gamma}{4}\sqrt{N_c^2-4} & -\Omega\sqrt{\frac{N_c^2-4}{N_c^2-1}} \\
\dots & 0 & \frac{\Gamma}{4}\sqrt{N_c^2-4} & 0 & \frac{-\Omega}{4}\sqrt{N_c^2-4} & 0 \\
\dots & \frac{\Sigma}{2\sqrt{2}}\sqrt{\frac{(N_c-3)(N_c-1)(N_c+2)}{N_c-2}} & \frac{N_c\Sigma}{\sqrt{2\left(N_c^2-4\right)}} & -\frac{\Sigma}{2\sqrt{2}}\sqrt{\frac{(N_c+3)(N_c+1)(N_c-2)}{N_c+2}} & 0 & 0 \\
\dots & \frac{2+2L_\beta+N_c(N_c-1)(\Lambda+2)}{2N_c} & 0 & 0 & -\frac{\Sigma}{2}\sqrt{\frac{N_c-3}{N_c-1}} & 0 \\
\dots & 0 & \frac{4+4L_\beta+N_c^2(\Lambda+2)}{4N_c} & 0 & \frac{-N_c\Sigma}{4} & 0 \\
\dots & 0 & 0 & \frac{2+2L_\beta+N_c(N_c+1)(2+\Lambda)}{2N_c} & \frac{\Sigma}{2}\sqrt{\frac{N_c+3}{N_c+1}} & 0 \\
\dots & \frac{-\Sigma}{2}\sqrt{\frac{N_c-3}{N_c-1}} & \frac{-N_c\Sigma}{4} & \frac{\Sigma}{2}\sqrt{\frac{N_c+3}{N_c+1}} & \frac{4+4L_\beta+N_c^2(2+\Lambda)}{4N_c} & \frac{-N_c\Sigma}{\sqrt{N_c^2-1}} \\
\dots & 0 & 0 & 0 & \frac{-N_c\Sigma}{\sqrt{N_c^2-1}} & \frac{1+L_\beta}{N_c}
\end{pmatrix},
\tag{29}
$$

$$\Gamma^{(2)}_{gg\to Q\bar{Q}g} = \frac{\alpha_s}{\pi} T_R$$

$$\times \begin{pmatrix}
N_c \ln(v_{15}v_{25}) & 0 & 0 & 0 & \frac{1}{\sqrt{2}} \ln\left(\frac{v_{45}}{v_{35}}\right) & 0 & \dots \\
0 & N_c \ln(v_{15}v_{25}) & 0 & 0 & 0 & \frac{1}{2} \ln\left(\frac{v_{45}}{v_{35}}\right) & \dots \\
0 & 0 & N_c \ln(v_{15}v_{25}) & 0 & 0 & 0 & \dots \\
0 & 0 & 0 & \frac{1}{4} N_c \ln\left(v_{15}^2 v_{25}^2 v_{35} v_{45}\right) & \frac{1}{2} N_c \ln\left(\frac{v_{15}}{v_{25}}\right) & 0 & \dots \\
\frac{1}{\sqrt{2}} \ln\left(\frac{v_{45}}{v_{35}}\right) & 0 & 0 & \frac{1}{2} N_c \ln\left(\frac{v_{15}}{v_{25}}\right) & \frac{1}{4} N_c \ln\left(v_{15}^2 v_{25}^2 v_{35} v_{45}\right) & 0 & \dots \\
0 & \frac{1}{2} \ln\left(\frac{v_{45}}{v_{35}}\right) & 0 & 0 & 0 & N_c \ln(v_{15}v_{25}) & \dots \\
0 & 0 & 0 & 0 & 0 & \ln\left(\frac{v_{25}}{v_{15}}\right) \sqrt{\frac{(N_c-3)(N_c-1)(N_c+2)}{2(N_c-2)}} & \dots \\
0 & 0 & 0 & 0 & \frac{1}{4} \ln\left(\frac{v_{45}}{v_{35}}\right) \sqrt{N_c^2-4} & \frac{N_c \ln\left(\frac{v_{25}}{v_{15}}\right)\sqrt{2}}{\sqrt{N_c^2-4}} & \dots \\
0 & 0 & 0 & 0 & 0 & \ln\left(\frac{v_{15}}{v_{25}}\right) \sqrt{\frac{(N_c+3)(N_c+1)(N_c-2)}{2(N_c+2)}} & \dots \\
0 & 0 & \frac{1}{\sqrt{2}} \ln\left(\frac{v_{45}}{v_{35}}\right) & \frac{1}{4} \ln\left(\frac{v_{45}}{v_{35}}\right) \sqrt{N_c^2-4} & 0 & 0 & \dots \\
0 & 0 & 0 & 0 & 0 & 0 & \dots
\end{pmatrix}$$

$$
\begin{pmatrix}
\dots & 0 & 0 & 0 & 0 & 0 \\
\dots & 0 & 0 & 0 & 0 & 0 \\
\dots & 0 & 0 & 0 & \ln\left(\frac{v_{45}}{v_{35}}\right)\frac{1}{\sqrt{2}} & 0 \\
\dots & 0 & 0 & 0 & \frac{1}{4}\ln\left(\frac{v_{45}}{v_{35}}\right)\sqrt{N_{\rm c}^2-4} & 0 \\
\dots & 0 & \frac{1}{4}\ln\left(\frac{v_{45}}{v_{35}}\right)\sqrt{N_{\rm c}^2-4} & 0 & 0 & 0 \\
\dots & \ln\left(\frac{v_{25}}{v_{15}}\right)\sqrt{\frac{(N_{\rm c}-3)(N_{\rm c}-1)(N_{\rm c}+2)}{2(N_{\rm c}-2)}} & \frac{\ln\left(\frac{v_{25}}{v_{15}}\right)N_{\rm c}\sqrt{2}}{\sqrt{N_{\rm c}^2-4}} & \ln\left(\frac{v_{15}}{v_{25}}\right)\sqrt{\frac{(N_{\rm c}+3)(N_{\rm c}+1)(N_{\rm c}-2)}{N_{\rm c}+2}} & 0 & 0 \\
\dots & N_{\rm c}\ln\left(v_{15}v_{25}\right)-\frac{1}{2}\ln\left(\frac{v_{15}^2v_{25}^2}{v_{35}v_{45}}\right) & 0 & 0 & \ln\left(\frac{v_{15}}{v_{25}}\right)\sqrt{\frac{N_{\rm c}-3}{N_{\rm c}-1}} & 0 \\
\dots & 0 & \frac{N_{\rm c}}{4}\ln\left(v_{15}^2v_{25}^2v_{35}v_{45}\right) & 0 & \frac{N_{\rm c}}{2}\ln\left(\frac{v_{15}}{v_{25}}\right) & 0 \\
\dots & 0 & 0 & N_{\rm c}\ln\left(v_{15}v_{25}\right)+\frac{1}{2}\ln\left(\frac{v_{15}^2v_{25}^2}{v_{35}v_{45}}\right) & \ln\left(\frac{v_{25}}{v_{15}}\right)\sqrt{\frac{N_{\rm c}+3}{N_{\rm c}+1}} & 0 \\
\dots & \ln\left(\frac{v_{15}}{v_{25}}\right)\sqrt{\frac{N_{\rm c}-3}{N_{\rm c}-1}} & \frac{N_{\rm c}}{2}\ln\left(\frac{v_{15}}{v_{25}}\right) & \ln\left(\frac{v_{25}}{v_{15}}\right)\sqrt{\frac{N_{\rm c}+3}{N_{\rm c}+1}} & \frac{N_{\rm c}}{4}\ln\left(v_{15}^2v_{25}^2v_{35}v_{45}\right) & \frac{2N_{\rm c}}{\sqrt{N_{\rm c}^2-1}}\ln\left(\frac{v_{15}}{v_{25}}\right) \\
\dots & 0 & 0 & 0 & \frac{2N_{\rm c}}{\sqrt{N_{\rm c}^2-1}}\ln\left(\frac{v_{15}}{v_{25}}\right) & \frac{N_{\rm c}}{2}\ln\left(v_{35}v_{45}\right)
\end{pmatrix}
$$

$$
+\mathbf{diag}\left(-i\pi N_{\rm c},\ -i\pi N_{\rm c},\ -i\pi N_{\rm c},\ -\frac{3}{2}i\pi N_{\rm c},\ -\frac{3}{2}i\pi N_{\rm c},\ -i\pi N_{\rm c},\ -i\pi\left(N_{\rm c}+1\right),\ -\frac{3}{2}i\pi N_{\rm c},\ -i\pi\left(N_{\rm c}-1\right),\right.
$$
$$
\left.-\frac{3}{2}i\pi N_{\rm c},\ -i\pi N_{\rm c}\right). \tag{30}
$$

In the next step, a special case of $p_3^\mu = p_4^\mu$ is considered . The obtained matrix has a block–diagonal form:

$$\Gamma_{gg\to Q\bar{Q}g}\left(p_3^\mu = p_4^\mu\right) = \frac{\alpha_{\rm s}}{\pi} T_R \times \begin{pmatrix} \Gamma_{\mathbf{3\times 3}} & & \\ & \Gamma_{\mathbf{2\times 2}} & \\ & & \Gamma_{\mathbf{6\times 6}} \end{pmatrix}, \tag{31}$$

where

$$\begin{aligned} \Gamma_{\mathbf{3\times 3}} \;=\; & \frac{1}{N_{\rm c}} \times \mathbf{diag}\left\{1 + \left(1 - N_{\rm c}^2\right) L_\beta + N_{\rm c}^2 \ln\left(v_{15} v_{25}\right) - i\pi N_{\rm c}^2\,, \right. \\ & 1 + L_\beta + N_{\rm c}^2 \left(1 - i\pi + \frac{\Lambda'}{2} + \ln\left(v_{15} v_{25}\right)\right), \\ & \left. 1 + \left(1 - N_{\rm c}^2\right) L_\beta + N_{\rm c}^2 \ln\left(v_{15} v_{25}\right) - i\pi N_{\rm c}^2, \right\}, \end{aligned} \tag{32}$$

$$\Gamma_{\mathbf{2\times 2}} = \begin{pmatrix} \frac{4 + 4L_\beta + N_{\rm c}^2\left(2 - 6i\pi + \Lambda' + 2\ln(v_{15} v_{25} v_{35})\right)}{4N_{\rm c}} & -\frac{N_{\rm c}}{4}\left(\Sigma' + 2\ln\left(\frac{v_{25}}{v_{15}}\right)\right) \\ -\frac{N_{\rm c}}{4}\left(\Sigma' + 2\ln\left(\frac{v_{25}}{v_{15}}\right)\right) & \frac{4 + 4L_\beta + N_{\rm c}^2\left(2 - 6i\pi + \Lambda' + 2\ln(v_{15} v_{25} v_{35})\right)}{4N_{\rm c}} \end{pmatrix}, \tag{33}$$

and

$$\Gamma_{\mathbf{6\times 6}} = \begin{pmatrix} \frac{1+L_\beta+N_c^2\left(1-i\pi+\frac{\Lambda'}{2}+\ln(v_{15}v_{25})\right)}{N_c} & \frac{1}{2\sqrt{2}}\sqrt{\frac{(N_c-3)(N_c-1)(N_c+2)}{N_c-2}}\left(\Sigma'+2\ln\left(\frac{v_{25}}{v_{15}}\right)\right) & \frac{N_c}{\sqrt{2}\sqrt{N_c^2-4}}\left(\Sigma'+2\ln\left(\frac{v_{25}}{v_{15}}\right)\right) & \dots \\ \frac{1}{2\sqrt{2}}\sqrt{\frac{(N_c-3)(N_c-1)(N_c+2)}{N_c-2}}\left(\Sigma'+2\ln\left(\frac{v_{25}}{v_{15}}\right)\right) & \frac{1+L_\beta+N_c(N_c-1)\left(1+\Lambda'+2\ln(v_{15}v_{25})\right)-i\pi N_c(N_c+1)+N_c\ln v_{35}}{N_c} & 0 & \dots \\ \frac{N_c}{\sqrt{2}\sqrt{N_c^2-4}}\left(\Sigma'+2\ln\left(\frac{v_{25}}{v_{15}}\right)\right) & 0 & \frac{4+4L_\beta+N_c^2\left(2-6i\pi+\Lambda'+2\ln(v_{15}v_{25}v_{35})\right)}{4N_c} & \dots \\ \frac{-1}{2\sqrt{2}}\sqrt{\frac{(N_c+3)(N_c+1)(N_c-2)}{N_c+2}}\left(\Sigma'+2\ln\left(\frac{v_{25}}{v_{15}}\right)\right) & 0 & 0 & \dots \\ 0 & \frac{-1}{2}\sqrt{\frac{N_c-3}{N_c-1}}\left(\Sigma'+2\ln\left(\frac{v_{25}}{v_{15}}\right)\right) & \frac{-N_c}{4}\left(\Sigma'+2\ln\left(\frac{v_{25}}{v_{15}}\right)\right) & \dots \\ 0 & 0 & 0 & \dots \end{pmatrix}$$

$$\begin{pmatrix} \dots & \frac{-1}{2\sqrt{2}}\sqrt{\frac{(N_c+3)(N_c+1)(N_c-2)}{N_c+2}}\left(\Sigma'+2\ln\left(\frac{v_{25}}{v_{15}}\right)\right) & 0 & 0 \\ \dots & 0 & \frac{-1}{2}\sqrt{\frac{N_c-3}{N_c-1}}\left(\Sigma'+2\ln\left(\frac{v_{25}}{v_{15}}\right)\right) & 0 \\ \dots & 0 & \frac{-N_c}{4}\left(\Sigma'+2\ln\left(\frac{v_{25}}{v_{15}}\right)\right) & 0 \\ \dots & \frac{2+2L_\beta+N_c(N_c+1)\left(2+\Lambda'+2\ln(v_{15}v_{25})\right)-2i\pi N_c(N_c-1)-2N_c\ln v_{35}}{2N_c} & \frac{1}{2}\sqrt{\frac{N_c+3}{N_c+1}}\left(\Sigma'+2\ln\left(\frac{v_{25}}{v_{15}}\right)\right) & 0 \\ \dots & \frac{1}{2}\sqrt{\frac{N_c+3}{N_c+1}}\left(\Sigma'+2\ln\left(\frac{v_{25}}{v_{15}}\right)\right) & \frac{4+4L_\beta+N_c^2\left(2-6i\pi+\Lambda'+2\ln(v_{15}v_{25}v_{35})\right)}{4N_c} & \frac{-N_c}{\sqrt{N_c^2-1}}\left(\Sigma'+2\ln\left(\frac{v_{25}}{v_{15}}\right)\right) \\ \dots & 0 & \frac{-N_c}{\sqrt{N_c^2-1}}\left(\Sigma'+2\ln\left(\frac{v_{25}}{v_{15}}\right)\right) & \frac{1+L_\beta+N_c^2(\ln v_{35}-2i\pi)}{N_c} \end{pmatrix}. \quad (34)$$

For the $N_{\mathrm{c}} = 3$ case, the last block becomes even simpler: $\Gamma_{\mathbf{6}\times\mathbf{6}} = \Gamma_{\mathbf{1}\times\mathbf{1}} \otimes \Gamma_{\mathbf{5}\times\mathbf{5}}$. After performing the limit $\Sigma' = 0$, matrices take the following form:

$$
\begin{aligned}
&\Gamma_{gg\to Q\bar{Q}g}\left(\Sigma' = 0\right) = \frac{\alpha_{\mathrm{s}}}{\pi} T_R \times \frac{1}{N_{\mathrm{c}}} \\
&\times \mathbf{diag}\left\{1 + \left(1 - N_{\mathrm{c}}^2\right) L_\beta + 2N_{\mathrm{c}}^2 \ln v_{15} - i\pi N_{\mathrm{c}}^2,\right. \\
&1 + L_\beta + N_{\mathrm{c}}^2 \left(1 - i\pi + \frac{\Lambda'}{2} + 2\ln v_{15}\right), \\
&1 + \left(1 - N_{\mathrm{c}}^2\right) L_\beta + 2N_{\mathrm{c}}^2 \ln v_{15} - i\pi N_{\mathrm{c}}^2, \\
&1 + L_\beta + \frac{N_{\mathrm{c}}^2}{4}\left(2 - 6i\pi + \Lambda' + 2\ln\left(v_{15}^2 v_{35}\right)\right), \\
&1 + L_\beta + \frac{N_{\mathrm{c}}^2}{4}\left(2 - 6i\pi + \Lambda' + 2\ln\left(v_{15}^2 v_{35}\right)\right), \\
&1 + L_\beta + N_{\mathrm{c}}^2 \left(1 - i\pi + \frac{\Lambda'}{2} + 2\ln v_{15}\right), \\
&1 + L_\beta + N_{\mathrm{c}}\left(N_{\mathrm{c}} - 1\right)\left(1 + \Lambda' + 4\ln v_{15}\right) - i\pi N_{\mathrm{c}}\left(N_{\mathrm{c}} + 1\right) + N_{\mathrm{c}} \ln v_{35}, \\
&1 + L_\beta + \frac{N_{\mathrm{c}}^2}{4}\left(2 - 6i\pi + \Lambda' + 2\ln\left(v_{15}^2 v_{35}\right)\right), \\
&1 + L_\beta + \frac{N_{\mathrm{c}}}{2}\left(N_{\mathrm{c}} + 1\right)\left(2 + \Lambda' + 4\ln v_{15}\right) - i\pi N_{\mathrm{c}}\left(N_{\mathrm{c}} - 1\right) - N_{\mathrm{c}} \ln v_{35}, \\
&1 + L_\beta + \frac{N_{\mathrm{c}}^2}{4}\left(2 - 6i\pi + \Lambda' + 2\ln\left(v_{15}^2 v_{35}\right)\right), \\
&\left. 1 + L_\beta + N_{\mathrm{c}}^2\left(\ln v_{35} - 2i\pi\right)\right\}. \qquad (35)
\end{aligned}
$$

#### 3.2.1. Analysis of the eigenvalues for $gg \to Q\bar{Q}g$

In this subsection, we perform an analogous analysis of the eigensystem for $gg \to Q\bar{Q}g$ to the case of $q\bar{q} \to Q\bar{Q}g$. The set of the eigenvalues is richer then in the scattering process of the quark and antiquark due to the larger colour basis. For $\theta = 90^\circ$, the real parts of the regularized eigenvalues are shown in Fig. 5 and the imaginary parts are shown in Fig. 6. The singular matrix in $\beta_{34}$ has a form of $\frac{i\pi}{\beta_{34}} \times \mathbf{diag}\left(-\frac{2}{3}, -\frac{2}{3}, \frac{1}{12}, \frac{1}{12}, \frac{1}{12}, \frac{1}{12}, \frac{1}{12}, \frac{1}{12}, \frac{1}{12}, \frac{1}{12}, \frac{1}{12}, \frac{1}{12}\right)$ in this case. One finds also one value of the leading small-$\beta$ behaviour of the eigenvalues, which is the same as in the quark channel

$$
\lambda^{\mathrm{sing}} = 6 \log \beta\,. \qquad (36)
$$

After the procedure of regularization (analogous to the $q\bar{q}$ scattering case), one can see some similarities for both the scattering angles. In the case of $\theta = 90^\circ$, the eigensystem consists of 6 different eigenvalues. The degenerate

eigenvalues are $\lambda_1 = \lambda_2$, $\lambda_3 = \lambda_4 = \lambda_5 = \lambda_6$ and $\lambda_8 = \lambda_9$. The real parts of the eigenvalues are nearly constant up to $\beta \approx 0.6$ and all the imaginary parts are constant in whole range of $\beta$. The results for $\theta = 30°$ are shown in Fig. 7 (the real parts of eigenvalues) and in Fig. 8 (the imaginary parts of eigenvalues). The singular part of the eigenvalues at $\theta = 30°$ is the same as for $\theta = 90°$. The degeneracy of the eigensystem is lower (the degeneracy between eigenvalues 4, 5, 6, 7 is reduced to the separate degeneracy $\lambda_3 = \lambda_4$ and $\lambda_5 = \lambda_6$). The real parts of eigenvalues are nearly flat for $\beta < 0.5$, then they grow rapidly. $\mathrm{Im}(\lambda_{10}^{30°})$ ($\mathrm{Im}(\lambda_{11}^{30°})$) is a growing (decreasing) function of $\beta$. The imaginary parts of the remaining eigenvalues are constant.

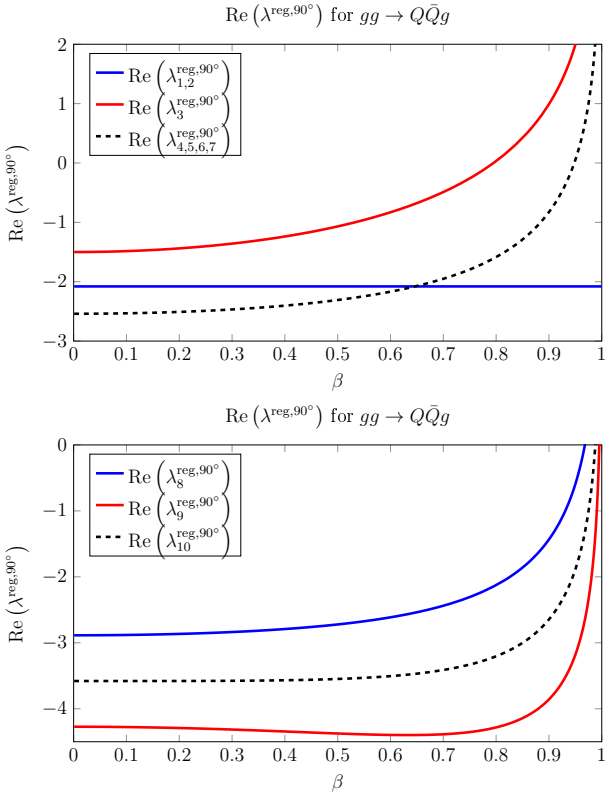


Fig. 5. The real parts of the regularized eigenvalues of $\tilde{I}_{\mathrm{S}}$ for $gg \to Q\bar{Q}g$ at $\theta = 90°$.

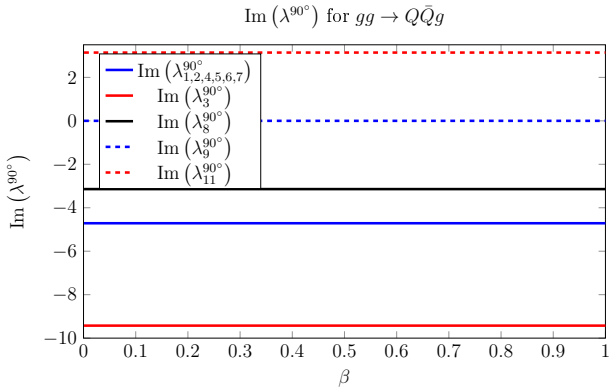


Fig. 6. The imaginary parts of the eigenvalues of $\tilde{\Gamma}_{\mathrm{S}}$ for $gg \to Q\bar{Q}g$ at $\theta = 90^\circ$.

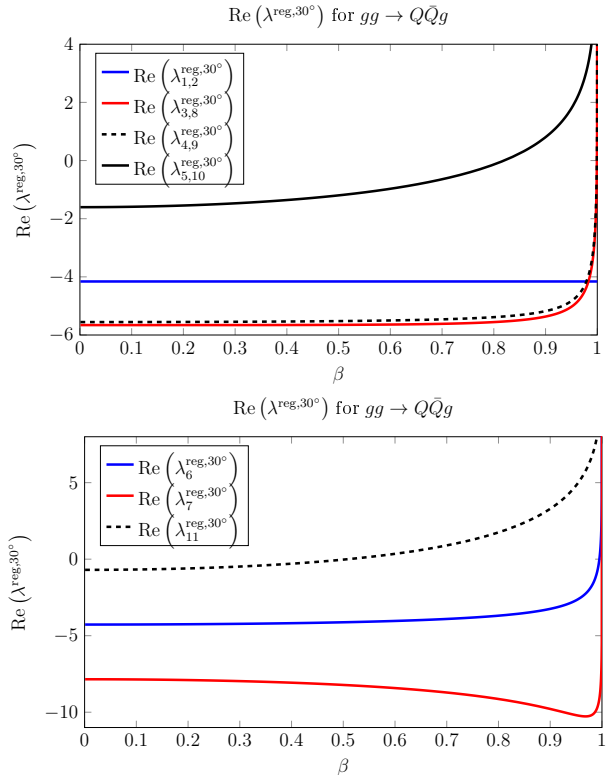


Fig. 7. The real parts of the regularized eigenvalues of $\tilde{\Gamma}_{\mathrm{S}}$ for $gg \to Q\bar{Q}g$ at $\theta = 30^\circ$.

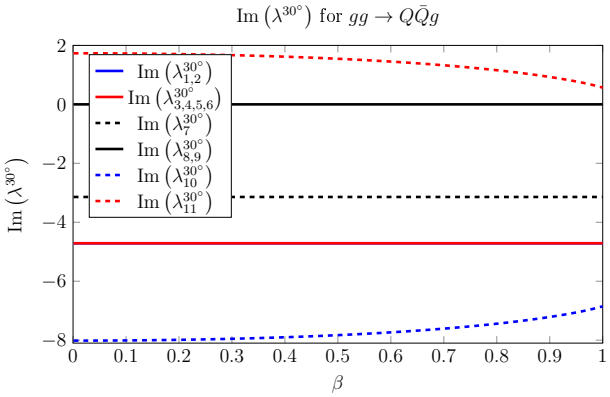


Fig. 8. The imaginary parts of the eigenvalues of $\tilde{\Gamma}_{\rm S}$ for $gg \to Q\bar{Q}g$ at $\theta = 30^\circ$.

## 4. Discussion and summary

In this paragraph, we compare the calculated regularized eigenvalues $\lambda_i^{\rm reg}$ of the SAD matrices to the SAD eigenvalues for processes $q\bar{q} \to Q\bar{Q}$ and $gg \to Q\bar{Q}$ in the small-$\beta$ region. Note that the full eigenvalues for $2 \to 3$ processes contain, in addition to the regular parts, a negative singular term $6 \log \beta$ for the $q\bar{q}$ and $gg$ channel. The logarithmic terms combine with the dominant regular terms into even larger negative terms of the eigenvalues, that is they lead to stronger effects of gluon radiation. For the $q\bar{q} \to Q\bar{Q}$ process, the real parts of the two at $\beta \to 0$ tend to $-1.5\frac{\alpha_{\rm s}}{\pi}$ and 0. Recall that for the case of $q\bar{q} \to Q\bar{Q}g$, the largest (negative) SAD eigenvalue reads ${\rm Re}\left(\lambda^{{\rm reg},90^\circ}\right) = -2.5\frac{\alpha_{\rm s}}{\pi}$ (for $\theta = 90^\circ$) and ${\rm Re}\left(\lambda^{{\rm reg},30^\circ}\right) = -5\frac{\alpha_{\rm s}}{\pi}$ (for $\theta = 30^\circ$). It means that the effect of soft gluon radiation for $q\bar{q} \to Q\bar{Q}g$ is almost two times stronger (the $90^\circ$ case) or three times larger (the $30^\circ$ case). In the gluonic case the radiation effects are even stronger. For $gg \to Q\bar{Q}g$, we obtained ${\rm Re}\left(\lambda^{{\rm reg},90^\circ}\right) = -4\frac{\alpha_{\rm s}}{\pi}$ (for $\theta = 90^\circ$) and ${\rm Re}\left(\lambda^{{\rm reg},30^\circ}\right) = -8\frac{\alpha_{\rm s}}{\pi}$ (for $\theta = 30^\circ$), so the radiation is enhanced by factors three and five, correspondingly, with respect to the $gg \to Q\bar{Q}$ process. The imaginary parts of eigenvalues cancel out in the $\beta \to 0$ regime, so we will not discuss them. These results imply that the soft gluon radiation is a source of enhanced corrections for the heavy-quark pair production in association with a gluon jet.

In this paper, we have derived the one-loop soft anomalous dimension matrices for $q\bar{q} \to Q\bar{Q}g$ and $gg \to Q\bar{Q}g$. We presented the SAD matrices for an arbitrary scattering angle $\theta$ of a clustered pair of heavy quark and antiquark with respect to the incoming parton axis in the CMS frame. We also analysed the spectrum of the eigenvalues of the SAD matrices in details for two kinematic configurations of $\theta = 90^\circ$ and $30^\circ$, performing explicit

numerical calculations of the SAD eigenvalues. Comparing the behaviour of the eigensystem of SAD matrices for processes $q\bar{q} \to Q\bar{Q}g$ and $gg \to Q\bar{Q}g$, one finds some similarities. For example, at $\theta = 90°$, there is a constant behaviour in $\beta$ for the imaginary part of eigenvalues in both reactions. When the kinematic configuration becomes less symmetrical (the $\theta = 30°$ case), the set of eigenvalues with a flat $\beta$-dependence is reduced. The obtained results are a step towards implementing the soft resummation procedure for $Q\bar{Q}$-jet production in hadron colliders, and improving accuracy of theoretical predictions.

The author would like to thank Prof. L. Motyka for the help in preparing this paper, Prof. M. Praszałowicz for valuable comments on the manuscript, Prof. A. Kulesza for the discussion, Prof. M. Sjödahl and R. Schäfer for the correspondence. This work was supported by the National Science Centre, Poland (NCN) grant DEC-2014/13/B/ST2/02486.

## REFERENCES

[1] A. Kulesza, L. Motyka, T. Stebel, V. Theeuwes, *J. High Energy Phys.* **1603**, 065 (2016) [arXiv:1509.02780 [hep-ph]].

[2] A. Broggio *et al.*, *J. High Energy Phys.* **1603**, 124 (2016) [arXiv:1510.01914 [hep-ph]].

[3] A. Broggio, A. Ferroglia, B.D. Pecjak, L.L. Yang, *J. High Energy Phys.* **1702**, 126 (2017) [arXiv:1611.00049 [hep-ph]].

[4] A. Kulesza, L. Motyka, T. Stebel, V. Theeuwes, *Phys. Rev. D* **97**, 114007 (2018) [arXiv:1704.03363 [hep-ph]].

[5] M. Sjödahl, *J. High Energy Phys.* **0812**, 083 (2008) [arXiv:0807.0555 [hep-ph]].

[6] M. Sjödahl, *Eur. Phys. J. C* **73**, 2310 (2013) [arXiv:1211.2099 [hep-ph]].

[7] J.C. Collins, D.E. Soper, G.F. Sterman, *Nucl. Phys. B* **261**, 104 (1985).

[8] N. Kidonakis, G.F. Sterman, *Nucl. Phys. B* **505**, 321 (1997) [arXiv:hep-ph/9705234].

[9] G.F. Sterman, *Nucl. Phys. B* **281**, 310 (1987).

[10] S. Catani, L. Trentadue, *Nucl. Phys. B* **327**, 323 (1989).

[11] N. Kidonakis, G. Oderda, G.F. Sterman, *Nucl. Phys. B* **531**, 365 (1998) [arXiv:hep-ph/9803241].

[12] R. Bonciani, S. Catani, M.L. Mangano, P. Nason, *Nucl. Phys. B* **529**, 424 (1998) [*Erratum ibid.* **803**, 234 (2008)] [arXiv:hep-ph/9801375].

[13] N. Kidonakis, R. Vogt, *Phys. Rev. D* **68**, 114014 (2003) [arXiv:hep-ph/0308222].

[14] M. Czakon, A. Mitov, G.F. Sterman, *Phys. Rev. D* **80**, 074017 (2009) [arXiv:0907.1790 [hep-ph]].

[15] V. Ahrens *et al.*, *J. High Energy Phys.* **1009**, 097 (2010) [arXiv:1003.5827 [hep-ph]].

[16] M. Cacciari *et al.*, *Phys. Lett. B* **710**, 612 (2012) [arXiv:1111.5869 [hep-ph]].

[17] N. Kidonakis, *Phys. Rev. D* **83**, 091503 (2011) [arXiv:1103.2792 [hep-ph]].

[18] M. Czakon, P. Fiedler, A. Mitov, *Phys. Rev. Lett.* **110**, 252004 (2013) [arXiv:1303.6254 [hep-ph]].

[19] M. Beneke, P. Falgari, S. Klein, C. Schwinn, *Nucl. Phys. B* **855**, 695 (2012) [arXiv:1109.1536 [hep-ph]].

[20] A. Kulesza, L. Motyka, *Phys. Rev. Lett.* **102**, 111802 (2009) [arXiv:0807.2405 [hep-ph]].

[21] A. Kulesza, L. Motyka, *Phys. Rev. D* **80**, 095004 (2009) [arXiv:0905.4749 [hep-ph]].

[22] W. Beenakker *et al.*, *Int. J. Mod. Phys. A* **26**, 2637 (2011) [arXiv:1105.1110 [hep-ph]].

[23] W. Beenakker *et al.*, *J. High Energy Phys.* **1201**, 076 (2012) [arXiv:1110.2446 [hep-ph]].

[24] W. Beenakker *et al.*, *J. High Energy Phys.* **1412**, 023 (2014) [arXiv:1404.3134 [hep-ph]].

[25] W. Beenakker *et al.*, *J. High Energy Phys.* **1605**, 153 (2016) [arXiv:1601.02954 [hep-ph]].

[26] S. Catani, D. de Florian, M. Grazzini, P. Nason, *J. High Energy Phys.* **0307**, 028 (2003) [arXiv:hep-ph/0306211].

[27] M. Bonvini, S. Marzani, C. Muselli, L. Rottoli, *J. High Energy Phys.* **1608**, 105 (2016) [arXiv:1603.08000 [hep-ph]].

[28] N. Kidonakis, *Phys. Rev. D* **82**, 054018 (2010) [arXiv:1005.4451 [hep-ph]].

[29] R. Schäfer, Bachelor Thesis, "The Colour Evolution of the $q\bar{q}g$ and $Q\bar{Q}g$ Production in the Quark Channel", 2017.

[30] T. Becher, M. Neubert, *Phys. Rev. Lett.* **102**, 162001 (2009) [*Erratum ibid.* **111**, 199905 (2013)] [arXiv:0901.0722 [hep-ph]].

[31] T. Becher, M. Neubert, *J. High Energy Phys.* **0906**, 081 (2009) [*Erratum ibid.* **1311**, 024 (2013)] [arXiv:0903.1126 [hep-ph]].

[32] T. Becher, M. Neubert, *Phys. Rev. D* **79**, 125004 (2009) [*Erratum ibid.* **80**, 109901 (2009)] [arXiv:0904.1021 [hep-ph]].

[33] M.H. Seymour, M. Sjödahl, *J. High Energy Phys.* **0812**, 066 (2008) [arXiv:0810.5756 [hep-ph]].